# Sorting clasts across laminated maar dunes, Kilbourne and Hunts Holes, New Mexico: comparisons to sorting across aeolian and fluvial bedforms

Dave W. Love, Allan Gutjahr, and Andreas Lazari

New Mexico Geology, v. 40, n. 2 pp. 45-60, Online ISSN: 2837-6420.
https://doi.org/10.58799/NMG-v40n2.45

*This page is intentionally left blank to maintain order of facing pages.*

# Sorting clasts across laminated maar dunes, Kilbourne and Hunts Holes, New Mexico: comparisons to sorting across aeolian and fluvial bedforms

*Dave W. Love*[1], *Allan Gutjahr*[2], and *Andreas Lazari*[3]
[1]New Mexico Bureau of Geology and Mineral Resources, New Mexico Institute of Mining and Technology, Socorro, NM 87801, *david.love@nmt.edu*, [2]New Mexico Institute of Mining and Technology, Socorro, NM 87801 (deceased), [3]Valdosta State University, Valdosta, Georgia, 31698

## Abstract

Unlike aeolian and fluvial grain-size distributions that vary longitudinally across bedforms, unimodal and multimodal grain-size distributions from individual laminae and thin beds across pyroclastic climbing dunes in exposures at Kilbourne and Hunts Hole maars remain similar, regardless of location on the dunes. By analogy with aeolian and fluvial deposits, distributions in the climbing-dune facies of these maar deposits are interpreted to be dominantly a fine-grained (0.15–0.35 mm) saltation mode, with removal of finer particles in suspension and incorporation of lesser creep fractions coarser than the saltation mode. In some laminae, coarser grains up to 10 mm in diameter are present. Like aeolian and some fluvial dune deposits, the saltation distributions may be described by the four parameters of hyperbolic distributions: slopes of asymptotes on fine and coarse sides of the distributions ($\varphi$ and $\gamma$), abscissa of the vertex where the two limiting lines of the hyperbola cross ($\mu$), and peakedness or the shape of the distribution near the mode ($\delta$). Sampled saltation distributions from dunes at Kilbourne and Hunts Hole maars have gentler asymptotic slopes, compared to aeolian and fluvial deposits, and have slightly smaller average $\mu$ and $\delta$. Removal of particles in suspension above individual laminae in the dunes appears to result in two kinds of logarithmic decreases in mass amounts on the fine side of the grain-size distribution curves. One type of decrease is very similar to steep decreases seen in aeolian and fluvial ripples and dunes, perhaps related to flow separation and suspension near the crests of the dunes. The other type is more gradual in laminae that have an order of magnitude more ash incorporated in the thin beds. If the saltation fraction is deposited by aeolian processes, impact threshold velocities at these two maars appear to be on the order of only 0.12 to 4 m/sec. Unlike experimental aeolian saltation fractions, which decrease in modal size and amount downwind in waning wind conditions, the pyroclastic saltation populations remain constant over a distance of at least 0.4 km at Kilbourne Hole, and the saltation populations at Hunts Hole are similar. Coarser-grained creep populations in the surge deposits appear to be more complex than their aeolian counterparts, and in some samples contain maximum grain sizes that are up to nine times coarser than the modal saltation values. The fractions coarser than the saltation mode exhibit a range of decreases in mass amounts and some samples appear to exhibit separate coarse modes similar to distributions seen in some aeolian granule megaripples and fluvial gravelly megaripples. In these pyroclastic surge deposits, coarse grains may have been added by fallout and entrained in thin beds mixed with saltating grains. However, if the coarse grains are mixed with a saltation population and emplaced as thin, dense, granular shear layers, the mechanisms responsible for deposition of discrete, continuous layers across large bedforms are unclear, perhaps analogous in some respects to granular shear layers in fluvial gravelly megaripples.

## Introduction

Phreatomagmatic processes forming various facies in tuffs along maar rims are interpreted to involve pyroclastic surges and dilute pyroclastic density currents generated under a variety of conditions, ranging from high-velocity, hot, dry, ash-laden pyroclastic density currents, to relatively cool, wet, mud-laden winds (Moore, 1967; Fisher, 1970; Waters and Fisher, 1971; Lorenz, 1973; Walker, 1983; Sheridan and Wohletz, 1983; Cas and Wright, 1987; Cole, 1991; Valentine and Fisher, 2000; White and Houghton, 2000; Houghton et al. 2000; Branney and Kokelaar, 2002; Gencalioglu-Kuscu et al., 2007; White and Ross, 2011; Sulpizio et al., 2014; Valentine et al., 2015; Breard and Lube, 2017), to even cooler, wetter pyroclastic density currents wherein steam condensed to water within the moving cloud and along the ground (e.g., Sheridan and Wohletz, 1983; Gencalioglu-Kuscu et al., 2007). Although volcanic eruptions have occurred subaqueously and through shallow groundwater (White and Houghton, 2000; Gencalioglu-Kuscu et al., 2007; White and Ross, 2011; Valentine et al., 2015), the co-eruption of quantities of sediment-laden water along with the pyroclastic surges and flows remains less investigated, even though many bedform descriptions were originally taken from fluvial sedimentology. Variables including temperature, density and concentrations of particles and dust within the ash clouds and a host of other properties make interpretations and models complex. The transport medium makes a big difference in the ways clasts are transported and sorted because rock clasts are more than 2000 times denser than air, whereas the same grains are only 1.8–2.6 times denser than water. In addition, the viscosities of the media are orders of magnitude different (Bagnold, 1979; c.f., Douillet et al., 2014). Thus, wind-driven ballistic impacts in air dislodge and move larger grains downwind as creep, but impacts in water do not. Other more massive and reverse-graded facies are likely generated as debris flows with interstitial fluids being either air or water. Mechanisms of transport and deposition of clasts in many types of pyroclastic deposits continue to be topics of investigation and discussion (Branney and Kokelaar, 2002; White and Ross, 2011; Andrews and Manga, 2012; Sulpizio et al., 2014; Douillet et al., 2014; Valentine et al., 2015; Breard and Lube, 2017 ). Recently, several researchers have begun wind-tunnel experiments that incorporate volcanic clasts and fine-grained "dust," coarser-grained clasts on the wind-tunnel bed, and variable bed-slope angles (Andrews and Manga, 2011, 2012; Doronzo and Dellino, 2011; Douillet et al., 2014; Breard and Lube, 2017).

The thin laminae and their grain-size distributions across pyroclastic dunes generate questions and interpretations concerning the processes that resulted in their formation and preservation. Many discussions describe and interpret the generation of bedforms and some types of laminae during passage of pyroclastic surges and dilute pyroclastic flows. Interpretations have included settling of particles from suspension (Dellino et al., 2008), by individual eddies at the base of pyroclastic surges (Andrews and Manga, 2012), high-frequency fluctuations in velocities along the ground surface (Sulpizio et al., 2014), passage of "plug flows" and "traction carpets," (Sohn 1997; Sohn and Chough, 1989; Douillet el al., 2015) and processes of "fluidization" (Wilson, 1980, 1984; Roche et al., 2004; Gravina et al., 2004; Girolami et al., 2015). Of particular interest is the transport, deposition, and formation of facies and bedforms at the base of pyroclastic surges and currents.

Some researchers approach the problem using principles of fluid dynamics and the physics of particle interactions within currents (Burgisser and Bergantz, 2002; Dellino et al., 2008; Andrews and Manga, 2012; Sulpizio et al., 2014). The basal layer where deposition takes place has been considered in terms of particle concentrations, particle-particle interactions, and rates of shearing within the layer (summarized in Sulpizio et al., 2014; basal granular-fluid flow of Breard and Lube, 2017). In contrast, a simpler set of approaches to gain an understanding of transport and sedimentation by wind, water, and debris flows, based on the basic physics of the ways the masses of individual particles are supported by either fluids or other particles, was offered by Bagnold (1941, 1966, 1968, 1973, 1977, 1979).

Fine particles transported by wind are supported in suspension by turbulent eddies; wind-blown sand grains are supported by episodic contact with the ground surface (saltation), and larger grains are bombarded and moved along the ground surface by impacts of saltating grains (short hops by large grains are called reptation; those that slide and roll are called creep). Grains avalanching down slip faces of dunes also move other grains in a down-gradient direction. Aeolian laminae are generated by at least three processes: the passing of low, wind-driven ripples across larger bedforms or planar surfaces, high-frequency fluctuations of wind speeds along the surface, and avalanching of grains down slip-face slopes of larger dune bedforms (Kok et al., 2012).

Sand grains saltate in water and go into and out of suspension similar to the way they do in turbulent air. Flowing water is more dense and viscous than air, so laminae may be generated by other processes, including planar sheet flow as well as passage of ripples and grain-avalanching off slip faces of ripples or dunes (Allen, 1982; Fourriere et al., 2010). Larger grains in flowing water move more by rolling and dragging along finer-grained beds, without ballistic impacts from other grains, particularly in low-gravel, low-gradient streams. Along gravelly channel bottoms, shear stresses within the bedload move larger clasts upward and they tend to remain at the surface, while smaller clasts move and aggrade beneath them (Bagnold, 1979). In addition, thin layers may be produced by the passage of hyperconcentrated flows or shearing processes within thin gravelly traction-sheets similar to debris flows. Also, along channel-margins, slower-flowing backwaters and eddies, and under waning flows, finer grains settle from suspension to form climbing ripples and plane beds with continuous laminations. These are very different from the volcanogenic forms discussed herein.

We studied pyroclastic dunes from the rims of Kilbourne and Hunts Holes in southern New Mexico in order to compare grain-size distributions from laminated and thin-bedded maar deposits with previously studied bedforms in wind-tunnel experiments and other aeolian deposits, and from waning flows in rivers. The nature of basal pyroclastic "granular-flow pulses" versus aeolian and fluvial saltation and thin gravelly "debris-flow" sheets leads to questions concerning mechanisms of deposition and the amounts of sediment-laden water generated by phreatomagmatic eruptions at these maars.

Kilbourne and Hunts Holes are 2.7 and 2.4 km-wide, 91 and 76 m deep, late Pleistocene maars located 42 and 47 km southwest of Las Cruces, New Mexico, formed by phreatomagmatic eruptions followed by significant post-eruptive subsidence (Stuart, 1981; Seager, 1987). These are typical maars with low, outward-sloping rims of ejecta cut by collapsed craters below the former ground level as defined by Wood (in Cas and Wright, 1987, p. 376–377) and Vespermann and Schmincke (2000). Kilbourne Hole maar has an age of 45±4 ka (M. Zimmerer, pers. commun., 2017; c.f., Gile, 1987). Hunts Hole remains undated but appears to be similar in age to Kilbourne Hole. The climate is semiarid and depth to groundwater is now approximately 100 m, so little alteration of the ejecta appears to have taken place below the zone of soil development, although commonly the deposits are partially consolidated. Only slight erosion of associated deposits has taken place on the edges of the crater rims. Excellent exposures of bedded and laminated deposits in the maar rims show a progression and repetition of several volcaniclastic facies in 4 to 20 meter vertical sections (Stuart and Brenner, 1979; Wohletz, 1980; Stuart, 1981; Seager, 1987; Bahar, 1991). Bedforms associated with these deposits include massive beds, planar beds, several types of dunes including progressive and regressive forms, and scours (Waters and Fisher, 1971; Stuart, 1981; Sheridan and Wohletz, 1983; Cas and Wright, 1987; Cole, 1991; Douillet et al., 2013). Some of the crossbedded dune deposits are similar to fluvial, pebbly sand crossbeds in subaqueous dunes (Fig. 1). Others are similar to aeolian ripples, dunes, and granule megaripples.

At Kilbourne Hole, Bahar (1991) showed that individual beds within pale, sandy, cross-bedded dune deposits along the maar rim are more than 90 percent reworked fluvial pebbly sand from underlying ancestral Rio Grande deposits, and that darker, coarser beds consist of 25–27 percent juvenile basaltic clasts and 58–71 percent ancestral Rio Grande pebbly sand. The exposed deposits also show many beds with soft-sediment deformation, as well as cratered structures formed by impacts of volcanic bombs that embedded themselves in laminated deposits, indicating water saturation in the deposits shortly after initial deposition. Accretionary lapilli, also characteristic of wet phreatomagmatic deposits, are present at more than one stratigraphic level. The preservation of individual laminae and thin beds within climbing dunes where individual laminae can be traced across parts or all of the

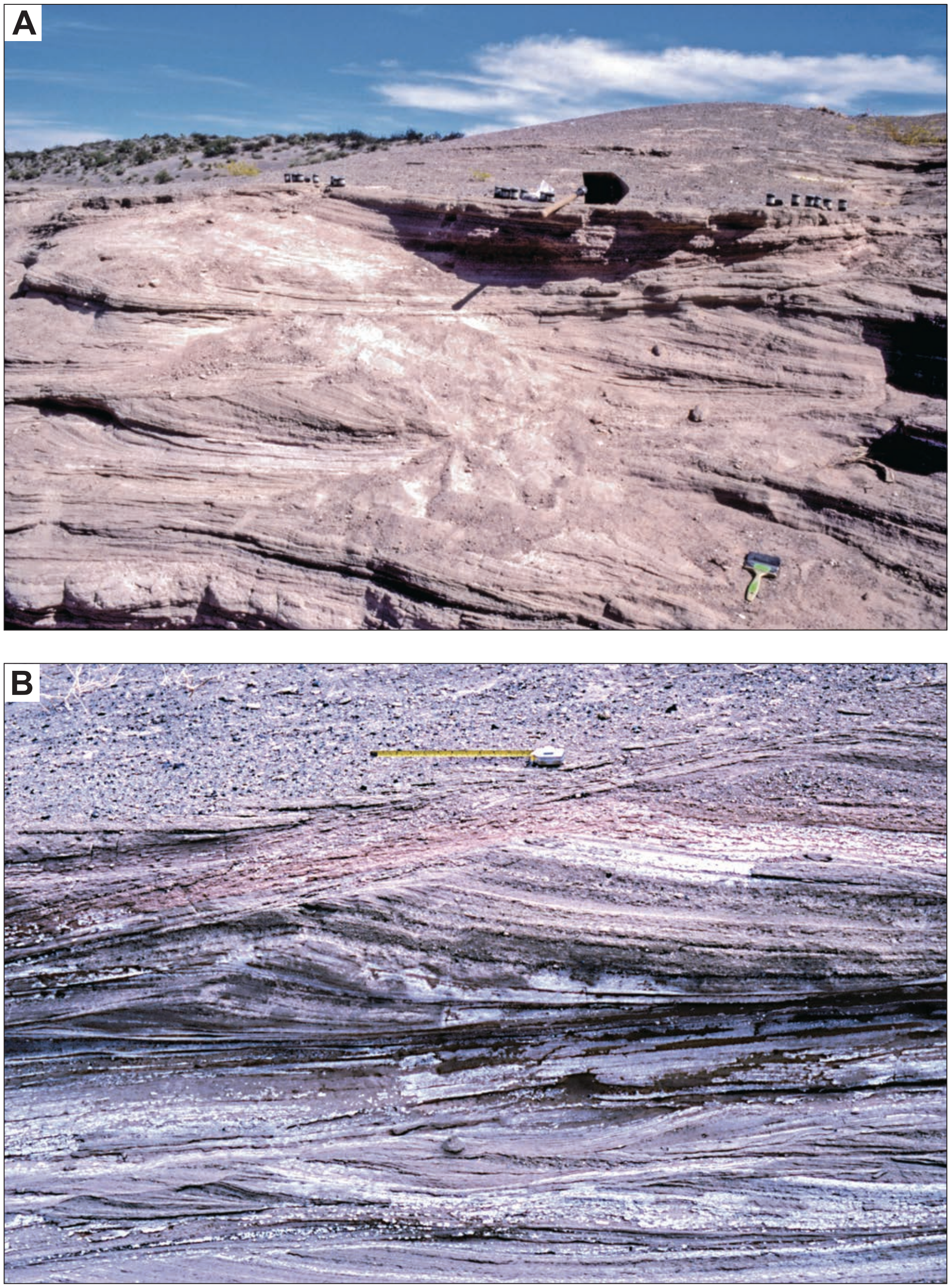


Figure 1. Pyroclastic sand-wave bedforms exposed at Kilbourne Hole maar. A) Exposure of crest, lee, bottomset, stoss, and crest of successive climbing dunes on the southeast side of Kilbourne Hole where samples were taken. Trenching tool for scale. B) Closeup of migrating stoss, crest, and lee bedsets (type b dune of Cole, 1991). Tape measure is extended 30 cm.

bedforms (i.e., types b and c sand waves of Cole, 1991; very different from dunes described by Douillet et al., 2013; Fig. 1) permits sampling and granulometric analysis of discrete depositional units. Granulometric analyses of volcaniclastic deposits in general are important to understand mechanisms of mobilization, transport, and deposition of clastic grains, and secondarily for purposes of classification of these types of deposits (Wohletz, 1980; Sheridan et al., 1987; Bahar, 1991; Wohletz et al., 1995; Gencalioglu-Kuscu et al., 2007). At Kilbourne Hole, sampling was done in low-amplitude climbing dunes (Stuart and Brenner, 1979; type c sand waves of Cole, 1991), in which stoss, lee, and bottomset beds are preserved during aggradation on the south and southwest exposures 1.8 to 2.2 km from the center of the crater and about 4 m above the base of the surge deposits. Following bedding terminology summarized by Reineck and Singh (1980), the smallest-scale depositional units in the dunes consist of laminae and thin beds (Figs. 1, 3).

In this paper we (1) describe Bagnold's (1937) illustrative technique and Barndorff-Nielsen's (1977, 1979) hyperbolic mathematical models to characterize grain-size distributions; (2) present the results of grain-size analyses of individual laminae from climbing dunes along the rims of Kilbourne and Hunts Holes; (3) compare these results with Bagnold's (1941) experimental aeolian deposits created under waning wind conditions and other reported aeolian megaripples, and with deposits in waning-flow fluvial dunes from the Rio Grande, (4) present hyperbolic models for some of the grain-size distributions and (5) speculate on the processes generating both the laminae and grain-size distributions.

## Methods

We sampled individual layers in dune bedsets that could be traced longitudinally over distances of a few meters because the dunes progressively climb down-gradient; stoss, crests, lee sides, and bottomsets are preserved. One particular bedset at Kilbourne Hole contains a pinkish clay coating that allows it to be traced laterally, so that adjacent bedsets above and below can be identified and sampled accordingly. In the climbing dunes we studied, crests progress down-gradient and increase in height, but due to thickened deposition on the lee slope and bottomsets, the bedsets shallow upward before the sequence tops out in nearly horizontal parallel laminae. Similar sequences of bedforms in the section may be interrupted by scour, with completely preserved bedforms above and below. We used the terminology shown in the Figure 3 field sketch, and sampled individual beds at locations indicated by letters on the sketch. Centimeter-scale samples of stoss, crest, lee, and bottomset beds of fine parallel laminae ranged in mass from 15–50 g. Coarse beds were sampled in masses as much as 1,400 g. We used quarter-phi-size brass sieves to determine the masses of grain sizes from 0.045 to 10 mm.

As an alternative to conventional probabilistic lognormal sedimentological methods, we use the graphical technique presented by Bagnold (1937, 1941) to illustrate grain-size distributions using log grain size–log mass frequency plots (discussed below). This illustrative technique is independent of assumed probabilistic models of distributions and is quasi-independent of sieves used as long as the sieve interval is relatively narrow. The technique also may show problems with aperture diameters in individual sieves if one assumes that the distribution curves should be smooth. In the following log-differential plots, it can be seen that some of the sieves are less than ideal, having mesh holes larger or smaller than labeled, such as the 0.212 mm sieve, producing downward deflections in the curves at 0.212 mm. Also note that the slopes of plots at the fine-grained ends (silt sizes) are likely influenced by the assumed size of the smallest fraction (0.001 mm). The illustrative technique has led to the formulation of hyperbolic probability distributions (Barndorff-Nielsen, 1977, 1979) that may be applied to aeolian and fluvial, and here to pyroclastic maar-rim deposits.

## Bagnold's illustrative technique and resulting models

Bagnold (1937, 1941) developed log-differential diagrams to illustrate grain-size distributions. He pointed out that sieves do not have ideal aperture sizes or uniform intervals between successive sieves. He also pointed out the large range in mass percentages caught on the sieves. In order to account for and normalize effects from non-ideal sieves and size intervals, the mass percentage for each size interval is divided by the difference in the logarithms of the sizes of the largest and smallest clast (in mm) in the interval. The resulting number is plotted using a logarithmic ordinate, with the logarithmic midpoint of the size interval as abscissa. Such diagrams show small size-grade amounts equitably with larger amounts, and because each interval is quasi-independent of other intervals, the shapes of portions of the curves remain similar even if portions of other sizes are added or subtracted. The illustrative technique is independent of any assumed probability model for the distribution.

Traditional lognormal probability distributions are parabolas on log-differential diagrams, but as Bagnold (1937, 1941; Bagnold and Barndorff-Nielsen, 1980) has shown, size distributions of many aeolian and fluvial deposits are hyperbolic in shape (Fig. 2). Furthermore, Bagnold (1941) indicated that for "regular" aeolian sands, the slopes of the lines on the coarse and fine sides of the distribution curves (asymptotic lines) approach limits of approximately 9 and 2.5 respectively ("regular" sands are those with size-grading curves that illustrate nearly linear slopes descending from a modal value of grain diameter).

Barndorff-Nielsen (1977) developed a family of mathematical equations for hyperbolic distributions using four parameters. Hyperbolic distributions can be generated in both deterministic and random ways, including being the product of infinite mixtures of lognormal distributions. Unlike the four moment descriptors commonly used in sedimentology (mean, standard deviation, skewness, and kurtosis), the four hyperbolic parameters can be used quantitatively in probability expressions to model grain-size distributions.

Barndorff-Nielsen et al. (1982) showed that the four parameters of hyperbolic size distributions varied longitudinally across a small aeolian dune. Love et al. (1987) showed that fluvial grain-size distributions were also location-dependent, and varied as flow waned. In addition, they showed that sorting processes take place on at least two scales, affecting the four hyperbolic parameters in different ways in a down-flow direction.

## Mathematical treatment of log-hyperbolic distributions

As developed by Barndorff-Nielsen (1977) and applied by Love et al. (1987), hyperbolic distributions are generalizations of normal distributions and require four parameters. For appropriate grain-size data, the logarithm of the grain diameter is assumed to have a hyperbolic distribution. By analogy with lognormal distributions, the grain size is thus said to be a log-hyperbolic random variable.

If $V = ln\ d$ (where $d$ is grain diameter), the probability density function of $V$ with four parameters is:

$$\ln f(V) = C_o - ([\delta^2 + (V - \mu^2)]^{1/2} (\varphi + \gamma))/2 + (V - \mu)(\varphi - \gamma)/2 \quad (1)$$

where $\mu$ is the abscissa of the point where the asymptotes cross, $\delta$ is a scale parameter influencing the sharpness of curvature of the peak, and $\varphi$ and $\gamma$ represent the slopes of the asymptotic lines of the hyperbola. $C_o$ is the ordinate of the point where the two limbs of the hyperbola cross above the vertex, and is a constant related to an expression involving $K_1$, which is a modified Bessel function of the third kind with index $\nu = 1$.

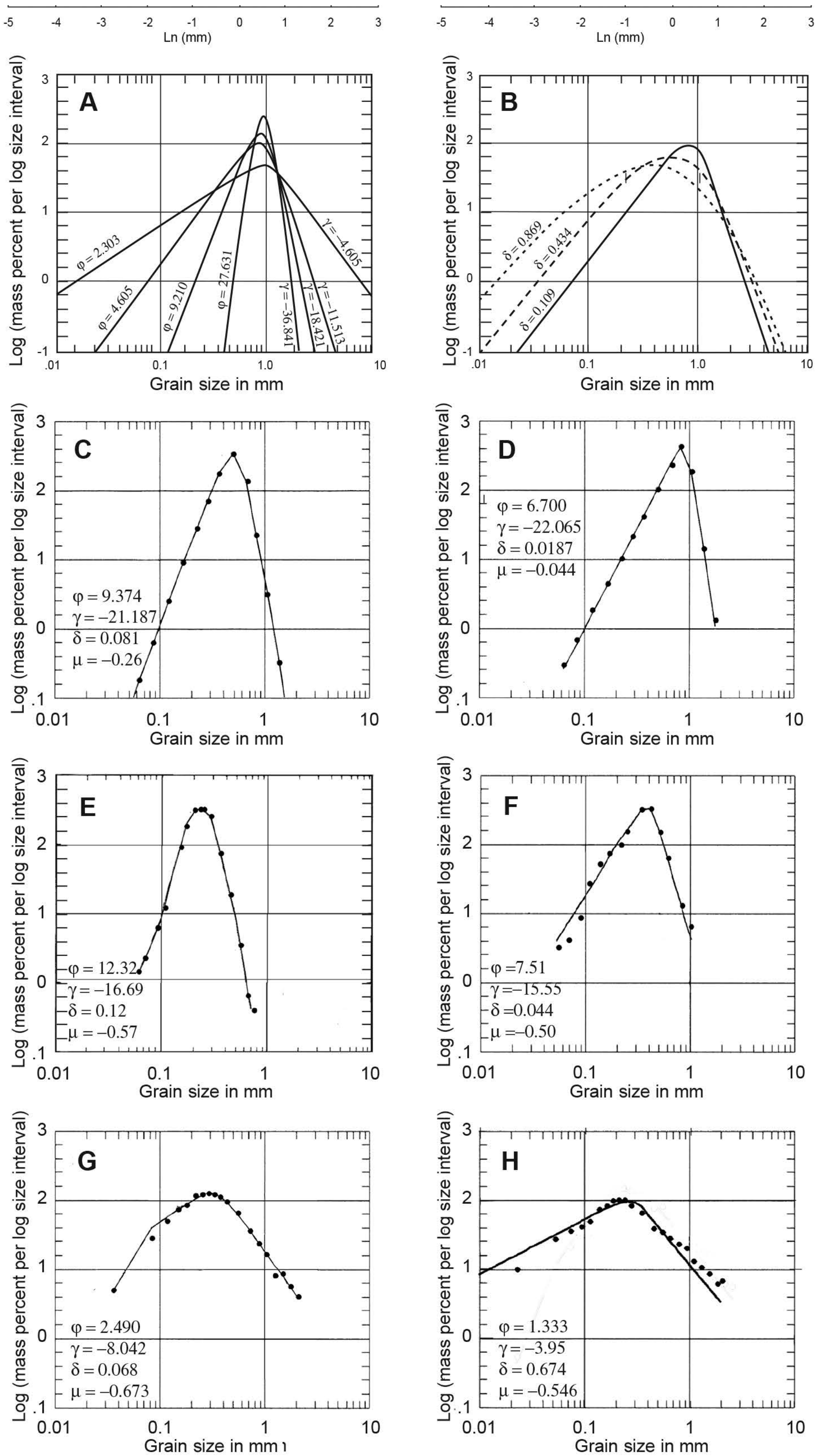


Figure 2. Hyperbolic models of grain-size distributions. A) Effect of slopes of asymptotes ($\varphi$, $\gamma$) on shapes of hyperbolic grain-size distributions. Upper abscissa scale is $\log_{10}$, lower scale is natural log. B) Effect of parameter $\delta$ on peakedness of hyperbolic distributions. C, D) Hyperbolic fits (lines) to grain-size data (dots) for aeolian deposits. Data from Bagnold (1941) are "regular" (C, saltation) and "skewed" (D, ultimate creep) modes, showing hyperbolic shapes and slopes of the coarse and fine limbs of the curves. Hyperbolic model parameters ($\varphi$, $\gamma$, $\delta$, and $\mu$) are $\log_{10}$ values. E, F) Fluvial examples are an upper foreset of a sandy dune, and a large ripple, both from the Rio Grande (Love et al., 1987). G, H) Pyroclastic-surge examples from bottomset and stoss locations from Kilbourne Hole deposits (v and t respectively in Fig. 3).

According to Barndorff-Nielsen (1977), $C_o$ can be calculated as follows:

$$C_o = \ln [\omega/\delta\kappa K_1(\delta\kappa)] \quad (2)$$

where

$$\kappa = (\varphi\gamma)^{1/2} \quad (3)$$

$$\omega = \frac{\varphi\gamma}{\varphi+\gamma} \quad (4)$$

If (1) is used to describe the behavior of $V = ln\ d$, the proportion ($P_i$) of grains with d between $d_{1i}$ and $d_{2i}$ can be calculated by letting $V_{1i} = ln\ d_{1i}$, $V_{2i} = ln\ d_{2i}$ and evaluating

$$P_i\ (\mu, \delta, \varphi, \gamma) = \int_{V_{1i}}^{V_{2i}} f\,(V; \mu, \delta, \varphi, \gamma)\ dV \quad (5)$$

If $ln\ d_{1i}$ - $ln\ d_{2i}$ is small, then the ratio $P_i/(ln\ d_{1i}\text{-}ln\ d_{2i})$ approximates the hyperbolic probability density.

The mode, or maximum value for the probability density function is given by

$$V_m = \mu + \delta\ (\varphi - \gamma)\ 2\varphi\gamma \quad (10)$$

The four parameters are estimated using a maximum likelihood iterative technique

$$MLE = \sum_{i=1}^{m} r_i \ln P_i\ (\mu, \delta, \varphi, \gamma) \quad (11)$$

where $r_i$ is the observed proportion of grains found in the range $d_{1i}$ to $d_{2i}$. We used the Rosenbrock hill-climbing method with constraints (Kuester and Mize, 1973) to approximate the integral for $P_i$.

For illustrative purposes, the abscissa on the data graphs presented here use a $\log_{10}$ rather than a natural log scale and $\mu$, the point on the abscissa where the two asymptotes cross, is left in $\log_{10}$ units rather than mm. Because one of the four parameters used in Barndorff-Nielsen's analysis is designated $\varphi$, we use $\varphi$ for the mathematical parameter and use the spelled-out term "phi-size" to distinguish the commonly used sedimentological units of sieve size. Figures 2A and B illustrate how the slopes of the two asymptotes ($\varphi$ and $\gamma$) affect the shape of the distribution, and how the scale parameter ($\delta$) affects the sharpness of the peak of the distribution.

Bagnold and Barndorff-Nielsen (1980) show that on log size-linear percent graphs, the hyperbolic distributions can be used to illustrate the properties of skewness and kurtosis commonly used to describe deviations from normal probability distributions.

# Comparisons of grain-size distributions from maar-rim, aeolian, and fluvial deposits

## Kilbourne and Hunts Hole bedforms and distributions

As Figure 3 shows, variability of size distributions is large from similar locations on a dune (such as stoss, crest, lee, or bottomset beds), but size distributions along individual beds are similar, despite location on the form. At most, lee-location beds tend to have slightly more rounded modal portions (Fig. 3: d, v) due to increased amounts in the 0.3 to 2 mm range relative to the adjacent stoss and bottomset samples. Some beds show unimodal hyperbolic distributions, but exhibit variable coarse and fine slopes. The decreases in masses of grains finer than about 0.2 mm have two types of slopes–steep slopes (Fig. 3: k, l, n, q) and gradual slopes (Fig. 3: a, e, g) (Stuart, 1981). Those with gradual slopes are apparently affected by a large (up to 33 percent) fraction of grains less than about 0.09 mm in diameter. Similarly, the coarse sides of the distributions have more than one type of slope, some steep, some gradual, and some extending subhorizontally with significant coarse fractions between 0.9 and 10 mm in size (Fig. 3: l, m, p). Many of the distributions have hyperbolic shapes in sand sizes, with additions of coarser fractions (Fig. 3: j, k). The coarser fractions may or may not be in separate modes (Fig. 3: k, l, m, p, q). In some cases the distribution on the coarse end is nearly flat over a wide range of sizes, and decreases in a "regular" manner on the fine side of the distribution (Fig. 3: m, p). Samples from similar locations along, above, and below the pink marker bed on the next well-exposed dune away from the crater (a few meters down-gradient) showed nearly identical size distributions. Samples from a smaller, more distal bedform 2.2 km from the center of Kibourne Hole showed similar unimodal distributions. In particular, the mode and the shape of the fine portions were nearly identical to the distributions observed from samples obtained closer to the center of the maar (e.g., Fig. 3: g, u, w).

At Hunts Hole, samples were taken from fine and coarse bottomset, stoss, crest, and lee positions along beds forming a large climbing dune with a progressively enlarged amplitude of over 3 m, similar to the one illustrated by Stuart (1981, fig. 3). Except for the coarsest fractions, the distributions along the fine-grained bed are similar, very "regular," and match the fine-grained distributions at Kilbourne Hole (Fig. 4). The coarse lee sample (Fig. 4F) shows a separate coarse fraction with a mode of 2.18 mm (mid-point), similar to some of the distributions from Kilbourne Hole samples (e.g., Fig. 3: k, n, o, q).

## Grain-size distributions from wind-tunnel experiments and other aeolian investigations

Although many studies of aeolian transport following Bagnold (1941) have addressed sand saltation and suspension of dust, few have examined the processes of creep or reptation (cf., Rice et al., 1995; Rasmussen et al., 1996; Butterfield, 1999; Zou et al., 2001; Dong et al., 2002; Namikas, 2003, 2006; Yizhaq, 2008; Duran et al., 2011; Kok et al., 2012; Qian et al., 2012; Farrell et al., 2012; Ho et al., 2014; Rasmussen et al., 2015; Valance et al., 2015; Mayaud et al., 2017). A literature search did not reveal other investigations replicating or expanding on Bagnold's (1941) investigations of creep in decreasing winds. Bagnold (1941) constructed a wind tunnel with a sediment trap to collect the creep fraction, and a ceiling that diverged downwind to decrease wind velocity (Fig. 5A). He spread sand with a broad range of sizes on the upper end of the tunnel, ran experiments at several wind velocities, and analyzed the amounts and grain sizes at down-tunnel locations. His experiments show that first, as wind slackens down gradient, the amount of

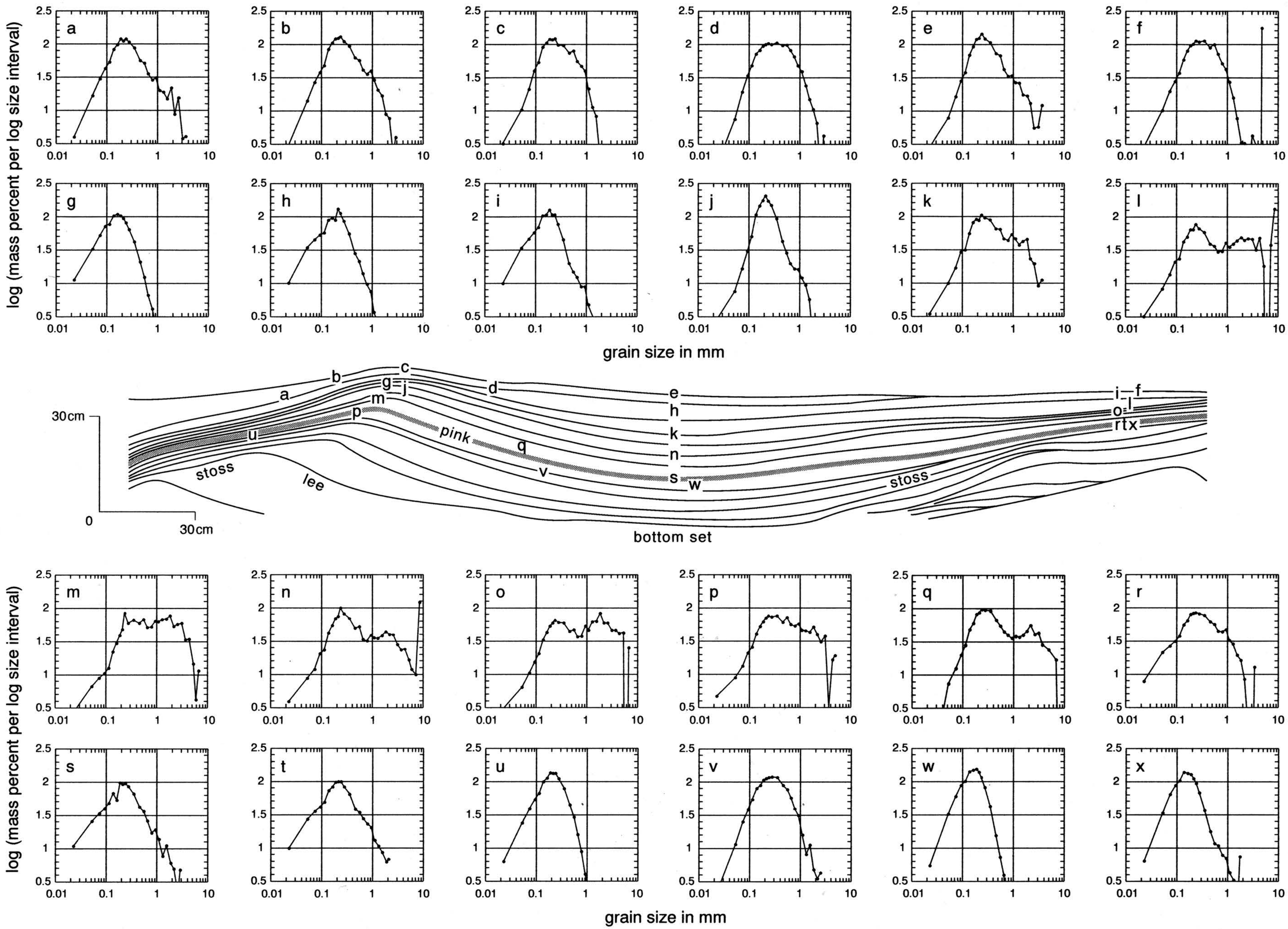


Figure 3. Labeled sketch of climbing-dune bedforms at Kilbourne Hole maar, and grain-size distributions from stoss, crest, lee, and bottomset locations. Sample locations for corresponding data plots are shown on the sketch. The bedforms were sampled on the southeast side of the maar, 1.8 km from the center. “Pink” on sketch refers to distinctive marker bed discussed in text.

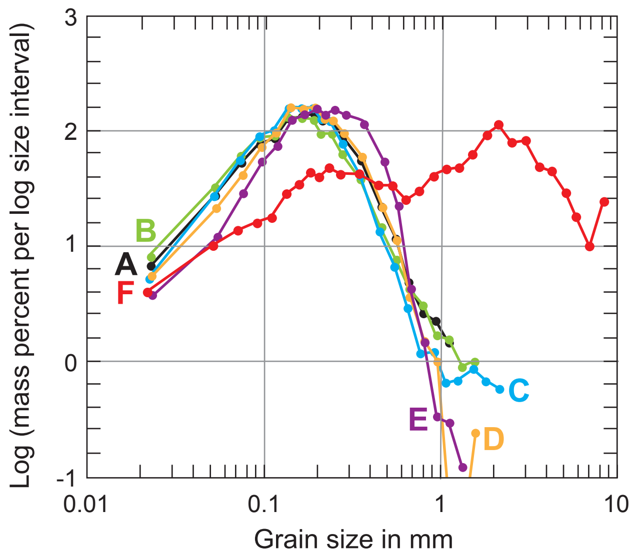


Figure 4. Grain-size distributions from Hunts Hole large climbing dune. A) Fine stoss; B) Fine crest; C) Fine lee; D) Medium-coarse stoss; E) Medium-coarse lee; F) Coarse lee.

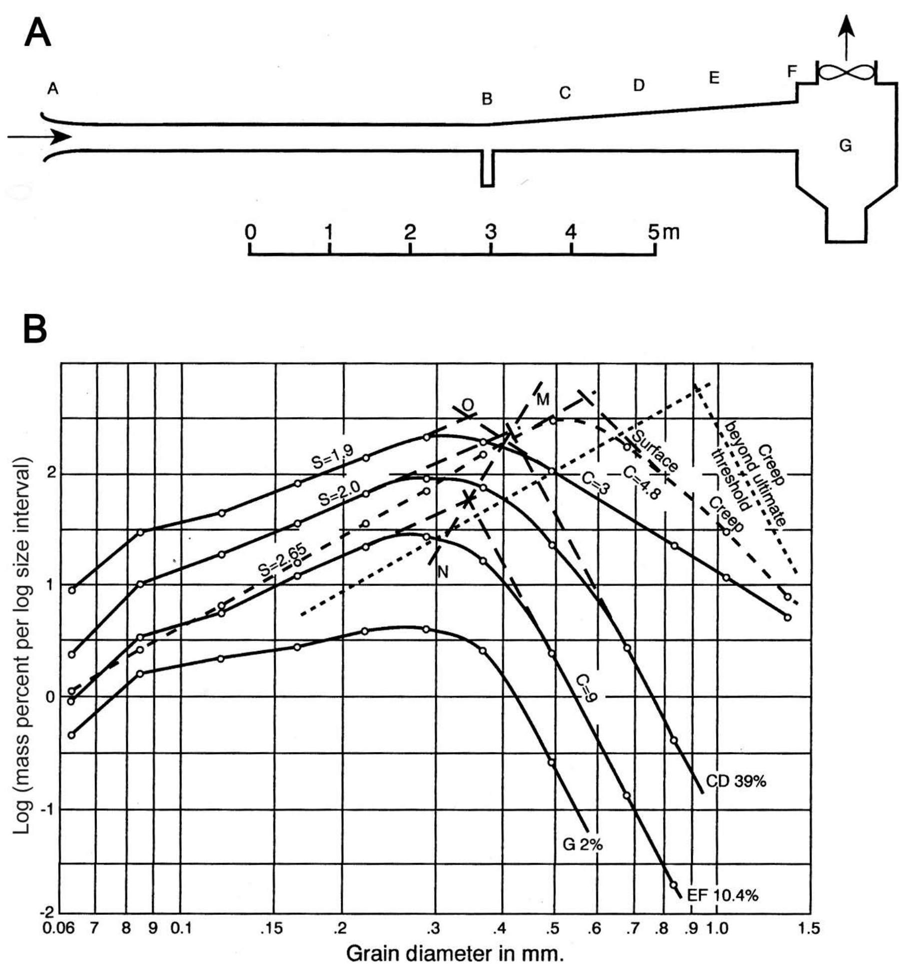


Figure 5. Sketch of Bagnold's wind tunnel and grain-size distributions from different locations after experiments under strong, but decreasing wind conditions (redrawn from Bagnold, 1941). A) Longitudinal section of wind tunnel showing creep trap ("B") and other sample locations along expansion reach of decreasing wind velocity. B) Grain-size distributions under strong wind conditions after only two minutes. Upper solid curve is beginning distribution. Individual curves below are labeled by sample locality in the wind tunnel, and percentage of beginning mass of sand mobilized when sample was taken. Slopes of the asymptotic lines on the fine and coarse sides of the distributions are indicated by "S =" and by "C =". Note that the modal grain size decreases downwind from M to N ("O" is the original sand mixture). The mode of the surface creep (dashed lines, from creep-trap samples) coarsens from 0.55 to about 0.9 mm in hypothetical "ultimate creep" (short dashed lines to right of others).

sand in transit decreases and the peaks of the size distributions get finer in proportion to the decreasing amounts (Fig. 5B). Initially, the wind-sorted bed had peak sizes smaller than that of the original mixture of sand. Later, as the experiment continued, the bed stabilized at coarser sizes, but with the same proportional decrease in size downwind. Second, the slopes of the hyperbolic lines increased to 9 for the coarse-end slope and near 2.5 for the fine-end slope (except for the sediment trap samples at the downwind end of the tunnel). Third, surface creep also resulted in a "regular" distribution, but had different asymptotic slopes (Fig. 2D; Fig. 5B; surface creep and creep beyond ultimate threshold). Thus, the creep distribution affects the size distribution of downwind deposits as the creep load overtakes them, increasing the amount of the coarsest sizes and decreasing the coarse-end slope. Strong winds shift the creep distribution to even coarser sizes and steepen the slope of the coarse end of the distribution.

Williams (1964) ran experiments on sorting of different shapes of sand grains saltating in a wind tunnel that did not expand downwind. The size distributions of grains closest to the floor of the tunnel (within 0.5 cm above the surface) were similar to those of Bagnold's creep fraction, while those saltating to greater heights were similar to Bagnold's "regular" saltation fractions. Williams concluded that initial surface size distribution and sphericity as well as the impact shear velocity gradient affected the size proportions in saltating grains.

Anderson (1990) and Anderson and Bunas (1993) investigated and modeled ripple-migration laminations described by Hunter (1977). Coarse grains move less than fine grains when impacted by other sand grains so they tend to concentrate near the crests of the ripples, whereas finer grains move farther and tend to gather in the lower lee faces and troughs of the ripples. This process leads to the generation of nearly planar, fine and coarse laminae as ripples move and climb downwind.

Rice et al. (1995) investigated the effects that three-sizes of saltating "impactor" sand grains had on beds of sand having three different sand sizes. As expected, they demonstrated that smaller sizes of sand on the bed were ejected at larger concentrations and speeds whereas larger grains were ejected at lower speeds and made only short "hops." They suggested that grains could be sorted by the distances they move, with smaller grains moving farther and more quickly downwind, leaving larger grains behind, while large grains moved more slowly over shorter distances, perhaps forming separate coarse populations.

Namikas (2003, 2006) investigated particle sizes, mass fluxes, and energy partitioning of saltating aeolian sand grains. He concluded that there is a constant kinetic energy level at liftoff for all sand size classes, which therefore reflects an inelastic impact regime between the saltating grains and the loose bed. Following Anderson (1990) and Rice et al. (1995), Namikas suggested that this provides a mechanism for size sorting wherein larger grains "hop" or reptate only short distances close to the bed whereas smaller grains take higher, longer trajectories. This may explain Bagnold's (1941) and Williams' (1964) results regarding sizes of "creep" along the floor of the expanding wind tunnel.

A lesser amount of literature describes and models aeolian ripples that are larger and coarser than normal aeolian ripples, known as "ridges," "aeolian megaripples," "gravel ripples," or "granule ripples." Among others Yizhaq (2008) and Qian et al. (2012) summarized what is known about granule ripples. Yizhaq (2008) presented a model for their generation, whereas Qian et al. (2012) measured wavelengths, heights and grain sizes in granule ripples generated in four areas of the Kumtagh Desert, China. The granule ripples had wavelengths between 0.31 and 26 m with heights between 0.015 and 1 m. The granule ripples had bimodal or trimodal grain-size distributions with fine modes between 0.105 and 0.125 mm and coarse modes at 2 mm. Some of these coarse ripples had a secondary coarse mode between 1 and 1.25 mm. None of the coarsest grains were more than 4 mm in diameter. The distributions shown by Qian et al. (2012) are similar to those that include very coarse fractions shown in Figures 3 and 4, but the bedforms and internal stratigraphy of the granule ripples are dissimilar to the pyroclastic deposits. Yizhaq's (2008) model generated granule megaripples by concentrating reptating coarse grains (<4 mm) on larger ripples and coalescing ripples into megaripples with coarse crests and finer stoss, lee, and bottomsets.

### Grain-size distributions from waning-flow bedforms of the Rio Grande

Love et al. (1985, 1987) illustrated grain-size distributions from subaqueous sandy ripples and dunes and gravelly megaripples from waning flow in the Rio Grande near Socorro, New Mexico. Many of the sandy distributions are either unimodal (Fig. 2C, D), or bimodal, which could be modeled by mixing two hyperbolic distributions. The dominant hyperbolic distributions are considered to be the saltation fraction, either forming sandy ripples or redeposited as the ripples cascade off slip faces of larger bedforms. Coarser sand and gravel fractions are not hyperbolic and are multimodal (illustrated below). It is possible that due to dispersive stresses of granular flow along the long stoss surfaces of the gravelly megaripples, the coarsest grains are concentrated at the surface of the bedforms and that grains below the surface are less coarse. In the sampled gravelly megaripples the very-fine-sand and silt fraction formed a separate mode even though most of the fine-grained fraction (between 0.06 and 0.2 mm) behaved similarly to the fine fractions of sandy fluvial dunes.

## Discussion

The maar-rim dunes we studied are consistently well-organized forms with multiple fine laminae and thin beds creating the bedforms. They have consistent grain-size distributions, suggesting some uniformity in mechanisms of transport and deposition. The modes of the main sand-sized fractions (0.15–0.35 mm) are rather fine-grained and are similar to both saltating wind-blown sand and fluvial dune crests. The steep and gradual types of linear decreases in amounts of fine fraction (less than about 0.2 mm), described earlier, suggest that fine grains are commonly only partially transported away in suspension, or are incorporated in laminae of dunes in more than one way. The differences in amounts of fine grains (at least an order of magnitude) in the two types is illustrated in Figure 6C (f and o versus n and q). Those distributions

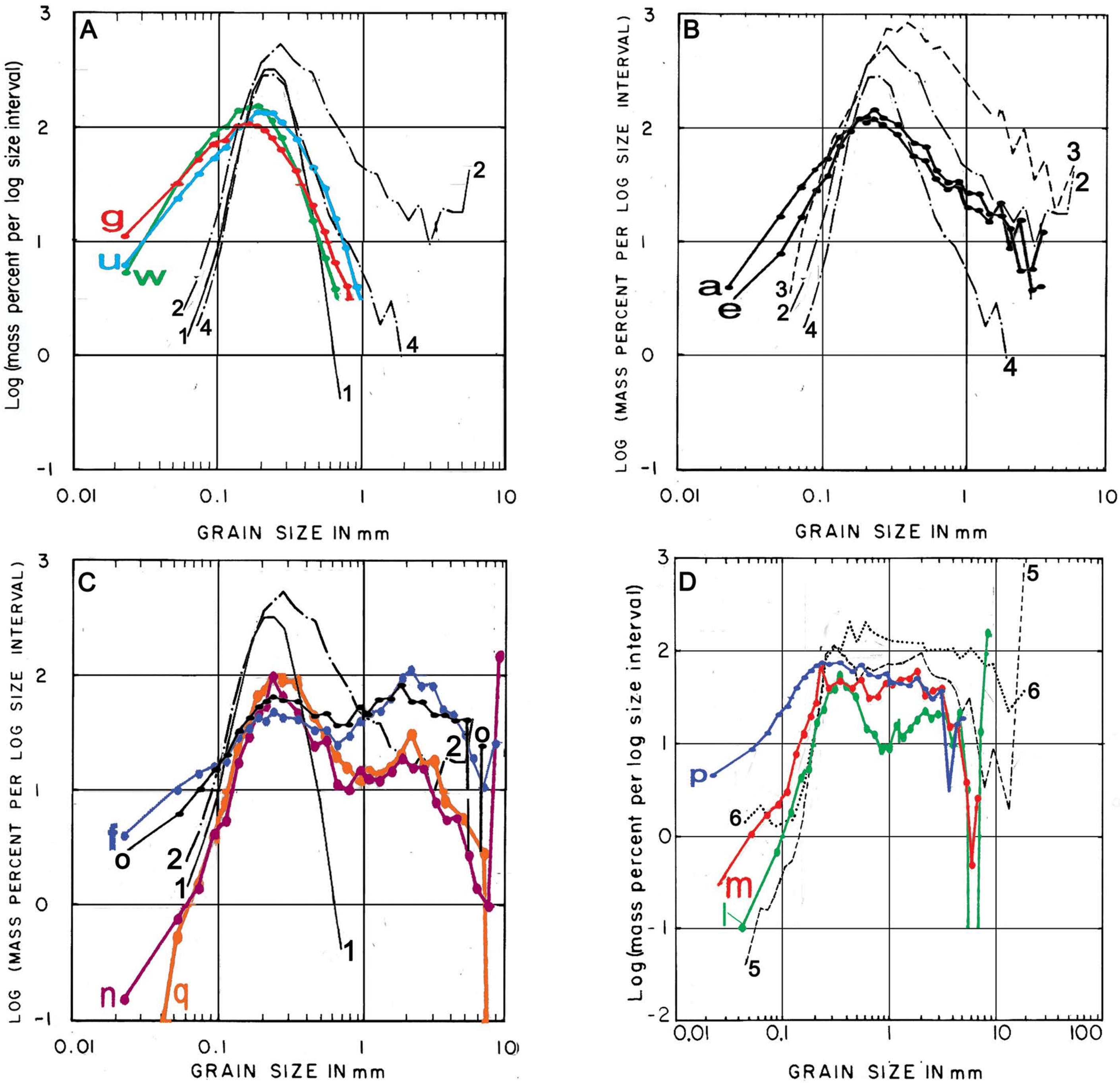


Figure 6. Comparison of grain-size distributions of upper foresets from sandy and pebbly megaripples in the Rio Grande (numbered lines, from Love et al., 1985, 1987), and laminated dune deposits from Kilbourne Hole (lettered lines– see Fig. 3 for sample locations). A) The volcaniclastic dune distributions are slightly finer grained than the fluvial dunes, and the shapes of the peaks are also different. The slope of the coarse-side fractions (*γ*) for the volcaniclastic deposits are similar to those for the fluvial sandy dunes. The slope of the fine-grained limbs (*φ*), however, are different from the fluvial examples. The amounts of fine sand and silt (probably fragmental ash) are nearly an order of magnitude more than in the fluvial examples. B) For the volcaniclastic samples, the modes are finer and the peaks broader than the fluvial examples, coarser grains are within the range of the fluvial examples, and the slopes of the finer fractions are more similar to the fluvial examples than in Fig. 6A. C) These curves were selected as examples of coarser-grained volcaniclastic deposits showing bimodal distributions. Included is a sample from Hunts Hole (curve "F" from Fig. 4). The modes for the saltation fractions are all between 0.2 and 0.3 mm. Coarser fractions (>0.9 mm) for the surge deposits in these examples appear to have a separate mode between 2 and 3.5 mm. D) Examples of coarser-grained deposits from Kilbourne Hole, together with two samples from coarser-grained fluvial megaripples from the Rio Grande (Love et al., 1985). Note that the distributions still have a saltation mode between 0.2 and 0.35 mm, with a flat or slightly peaked distribution from 1 to about 6 mm.

showing relatively large amounts of fine sand and silt (gradual fine-end slopes) are distinctly different from fluvial sandy megaripple deposits. Other distributions show a substantial decrease in sand and silt smaller than the modes, similar to decreases seen in fluvial sandy dune deposits (e.g., Fig. 6C, D).

Two observations may bear upon the question of why there are two types of decreases on the fine end of the hyperbolic distributions. First, low amounts of fines appear to correlate with a well-defined gravel mode that makes up less than half of the whole distribution (e.g., Fig. 6C: n and q). Second, if one considers flow separation and attachment similar to fluvial examples, perhaps both flow separation and movement of a coarser gravel mode could increase suspended load so less ash (particularly in lee and bottomset positions) is deposited down-gradient.

Considering an aeolian analogy for deposition of the pyroclastic deposits, the distributions may be explained as mixtures of saltation and one or more coarse (possibly creep) populations. The data are suggestive, but we certainly cannot prove that these populations are generated in such an analogous manner, or that other mechanisms of sorting are not taking place. The variability of fine and coarse slopes of the saltation populations suggests that the processes of saltation impacts, producing short hops for larger grains and longer flights for smaller grains, are only partially initiated and not as complete as the processes resulting from aeolian and fluvial transport. The amounts of fine grains incorporated in the saltation fraction may also depend on the concentration of dust near the surface during transport.

The small size range of the fine mode (between 0.125 and 0.350 mm) of the putative "saltation" fraction is perhaps surprising, considering the documented turbulence of pyroclastic density currents (Moore, 1967; Thorarinsson, 1967; White and Houghton, 2000). However, the important part of the pyroclastic cloud from a depositional standpoint is near the ground surface, where velocities go to zero and basal shear is set up. From Bagnold's (1941) and Anderson and Hallet's (1986) work, at ambient atmospheric conditions of temperature and pressure, the calculated critical-impact shear stress for saltating grains would be on the order of only 0.02 to 0.05 $N/m^2$, and the impact threshold velocity would be on the order of 0.12 to 2 m/sec. Douillet et al. (2014) calculated velocities between 1.26 and 3.95 m/sec to drive saltating granules (2–4 mm) of scoria in their wind-tunnel experiments, depending on pressure and temperature of the atmosphere within the pyroclastic currents. Following Walker (1984), both the climbing aggradation of lamina in the bedforms and the rather small dominant size of the saltation fraction suggest wind speeds near the ground may not have been substantial, or that other factors (such as moisture or abundant suspended dust) were modifying the depositional conditions.

In the dunes we sampled, the mechanisms sorting the coarser grains did not produce the uniform distributions exhibited by the finer mode, suggesting that processes sorting coarse grains are not as uniform, continuous, or as long-lasting as those in normal aeolian dunes. Coarse grains may have been added initially by fall out of ejecta, but the grains have been entrained in the transporting medium and deposited with the rest of the grains. Coarse modes are up to nine times larger than fine modes, possibly suggesting that large saltating grains played a dominant role in movement of the creep contribution to the coarse side of the grain-size distribution.

However, the incorporation of grains as large as 1 cm in diameter raises questions about mechanics of transport and deposition of the grains. First, aeolian creep and reptation of coarse grains requires saltating grains to dislodge and drive them along the surface. The coarsest of the saltation grains are 2–3 mm in diameter and are only a small fraction of the total, while the modes of the saltating population are less than a tenth as large, so how many of these grains must frequently impact the larger grains to drive them along? Second, if the decrease on the coarse end of the saltation fraction is due to lessening reptation of increasingly coarse grains, why is there a separate increase in even coarser grains (in samples with distinct coarse modes, including some with more coarse mode than saltation mode)? Third, are both the saltation and coarser populations produced during the same transport episode, or might they be inherited from separate processes? For example, could the saltation fraction and incorporated amount of fines be generated during part of an episode of pyroclastic flow, while the coarser fraction is generated as a thin debris flow that incorporates the saltation fraction too? Fourth, if the proposed debris-flow mechanism is viable, how does it follow bedform topography rather than concentrate along bottomsets? Is it dry or water-saturated? If possible, tracing individual beds over longer distances may provide evidence for "downwind" sorting.

Yet, similar size distributions from different locations in the climbing-dune facies of the maars at Kilbourne and Hunts Holes argue for similar depositional conditions and mechanisms. These mechanisms must be set up at the base of the pyroclastic cloud without regard for variations in velocities within the clouds, and must be maintained over distances of at least 0.4 km. Such conditions must have been maintained at a nearly constant threshold shear velocity and critical shear stress over distances at least on an order of hundreds of meters, producing nearly identical sorting. Additional wind-tunnel experiments would probably provide stronger evidence for these mechanisms under dry base-surge conditions. The range in amounts of the coarse fraction(s) suggests that the mechanism for transporting and depositing coarse grains does not depend on ballistic-impact drivers.

Considering that many historic phreatomagmatic eruptions also disperse large amounts of water, a water-transported analogy should be considered as an alternative for deposition of the pyroclastic-surge dunes. Clearly the bedforms are different from "normal" subaqueous dunes and ripples. However, some of the grain-size distributions are remarkably similar to distributions from bedforms deposited in the Rio Grande (Fig. 6). The sand fractions of the surge deposits coarser than the modes are similar to fluvial sandy dunes; some have steep decreases in amounts of coarser grains, whereas others have larger, variable amounts of coarser grains (Fig. 6A, B). The coarse sand-granule-small pebble fractions may derive from a separate mode (Fig. 3: l, n, o, q; Fig. 6B, C, D), which is also similar to distributions observed in some fluvial deposits (c.f., Love et al., 1985, 1987). The fact that most of the sand fraction in the surge deposits is derived from reworked ancestral Rio Grande deposits might indicate that the distribution is partly inherited, but the sorting must still take place under conditions of transport and deposition in the bedforms as they develop, and fine-grained clasts must still be winnowed away in a log-hyperbolic fashion.

Individual laminae or thin beds were deposited on top of the previous layers with minimal reworking of the underlying layer (i.e., coarse clasts, if present, stay within the previously deposited layer). If the dunes with their thin beds were laid down by shallow moving water, the implication would be that the water depth was at least as much as the height of the dunes, but that seems extremely unlikely. One could envision that an individual lamina could be laid down by an individual pulse of shallow, muddy water, hyperconcentrated flow, or a thin, wet debris flow driven laterally by hydromagmatic explosions and/or cloud collapse. One could envision runout zones similar to those at distal positions of alluvial fans where muddy water, hyperconcentrated flows, and debris flows spread into sheet flows producing thin laminated bedsets.

The water could come out of the developing crater as steam-driven pulses with incorporated sand from underlying ancestral Rio Grande deposits, or from condensation of water from clouds of steam moving away from the crater. The former condition would explain the erosion, transportation, and deposition of these sandy deposits, but the latter mechanism would still need to explain how adequate amounts of sand and coarser grains could fall out of clouds, be entrained by a wet fluid, and make consistent bedforms and grain-size distributions over broad areas.

Bagnold (1977) showed that in flowing water, the bedload transport rate decreases as an inverse function of the ratio of flow depth (Y) to bedload grain size (D), Y/D, so that where flows spread out and Y becomes shallow, larger clasts are deposited and the size of transported clasts decreases down gradient as Y decreases. However, if the coarsest fractions are added from ballistic fallout, large clasts may not decrease solely by mechanisms related to transport in flowing water. If the coarse grains are transported in thin debris flows, they would tend to move toward the free surface and toward the front of the flows (Bagnold, 1977), perhaps increasing the lateral extent of coarse grains. If each blast of hypothetical flowing water wanes at each location and away from the constructional maar rims, why are sandy ripples and fine-grained plane beds, so pervasive in sandy bedforms in waning fluvial-flow regimes (e.g. Allen, 1982; Love et al., 1987), not abundant? Probably because such a mechanism did not happen. If the saltation and larger grain-size fractions are mixed together to form laminae across the dunes, is it possible that thin, wind-driven, wet debris flows only a few particles thick, incorporating larger grains as well as saltation populations, could move across and deposit laminae uniformly on climbing dunes? Wet debris might be able to stick to and not erode previously formed topography better than dry, wind-driven avalanches. After all, muddy debris is a small step beyond mud-encrusted grains (pink layer and accretionary lapilli) known from these deposits.

Bimodal grain-size distributions of pyroclastic deposits have been reported from many other volcanoes, such as Mount St. Helens, Washington (Rowley et al., 1985), Campi Flegrei, Italy (Dellino et al., 2004), Cora Maar, Anatolia (Gencalioglu-Kuscu et al., 2007), Tungurahua, Ecuador (Eychenne et al., 2012), and Hekla volcano, Iceland (Janebo et al., 2018). None of these bimodal distributions is attributed to more than one mode of transportation and deposition. Instead, most of the distributions are within proximal massive or reverse-graded deposits and attributed to direct settling from pyroclastic density currents.

## Hyperbolic fits to aeolian, fluvial, and pyroclastic dune deposits

Where aeolian and fluvial saltation populations and pyroclastic-surge grain-size distributions appear to be unimodal hyperbolic distributions (Figs. 3, 6A, 6B), hyperbolic curves may be fitted to them (Fig. 2). A wide range in the four model parameters is indicated, particularly in the slopes of the asymptotes and peakedness ($\varphi$, $\gamma$, and $\delta$). The parameters $\varphi$ and $\gamma$ for aeolian distributions are consistently larger (steeper slopes) than for the pyroclastic-surge dunes. Fluvial distributions show a wider range in $\varphi$ and $\gamma$ (particularly $\gamma$) than aeolian distributions, but not as broad as pyroclastic dune distributions. Parameters $\delta$ and $\mu$ for aeolian distributions are only slightly larger and smaller, respectively, than for surge distributions (Fig. 2). If more than one population is present, two or more curves may be suggested (Figs. 3, 6). However, because the coarse population is never found by itself without the finer population, we have not determined the nature of the coarse population(s), or the nature of the overlap between the two suggested distributions. Do bimodal distributions reflect mixtures of two continuous, overlapping distributions, as Bagnold (1941) interpreted for bimodal aeolian sands, or are they truncated at either coarse or fine ends due to changes in transport and depositional mechanisms? In waning flow in the Rio Grande, small bedforms overtook larger bedforms to mix grain-size populations, but there is no evidence of small bedforms preserved in the pyroclastic-surge dunes.

An iterative technique to obtain best-fit estimates for two overlapping hyperbolic distributions was not developed here. It is straightforward, however, to mix two hypothetical distributions with specified parameters to construct bimodal distributions (Fig. 7). Such combinations can clearly mimic bimodal distributions from Kilbourne Hole, Hunts Hole, or from other pyroclastic deposits such as those mentioned above. In previous interpretations of "base-surge" grain-size distributions (Wohletz, 1983; Bahar, 1991; Wohletz et al., 1995), as many as five physical processes were invoked to explain inferred mixtures of lognormal populations as combinations of ballistic, rolling, saltation, and suspension populations. However, similar distributions may be reconstructed by combining just two hyperbolic distributions. This illustrates the hazard of interpreting populations based on assumptions about models and the difficulty of interpreting transport mechanisms solely from multiple lognormal fits to granulometric data.

## Conclusions

We compared grain-size distributions from laminae in pyroclastic-surge dunes from maar rims at Kilbourne and Hunts Holes with distributions from aeolian and fluvial deposits, and illustrated the log-differential nature of grain-size distributions of these laminae. We

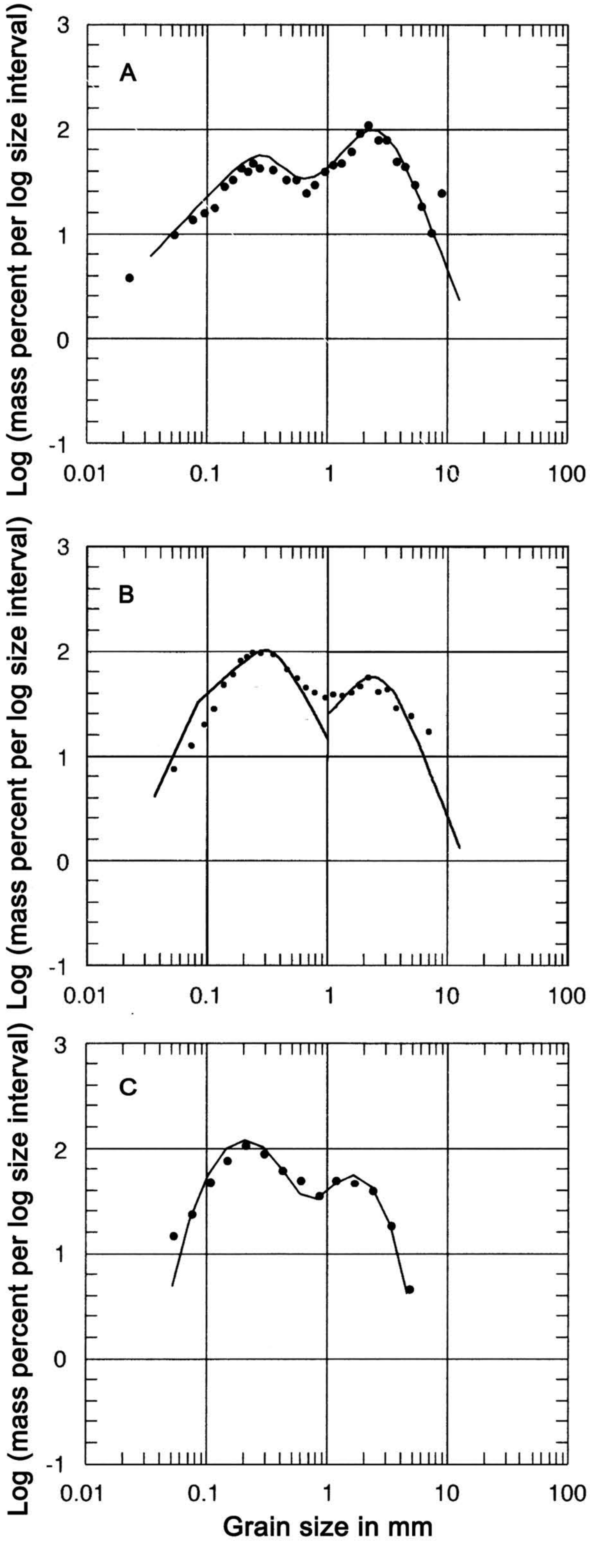


Figure 7. Combined hyperbolic distributions (lines) that mimic bimodal data (points) from base-surge deposits. A) Mixture of two distributions that reproduce a bimodal distribution from Hunts Hole (mix 42 percent $\varphi$ = 1.228, $\gamma$ = -1.718, $\delta$ = 0.307, $\mu$ = -.548 with 58 percent of $\varphi$ = 2.17, $\gamma$ = -3.32, $\delta$ = 0.569, $\mu$ = 0.326). B) Mixture of two distributions that reproduce a bimodal distribution from Kilbourne Hole (mix 66 percent $\varphi$ = 2.490, $\gamma$ = -8.042, $\delta$ = 0.068, $\mu$ = -0.673 with 34 percent of $\varphi$ = 2.17, $\gamma$ = -3.32, $\delta$ = 0.569, $\mu$ = 0.996). C) Mixture of two hyperbolic distributions that reproduce a bimodal distribution from Kilbourne Hole (data from Wohletz (1980) sample 8 A1; half phi-size sieve intervals (mix 29 percent of $\varphi$ = 6.05, $\gamma$ = -19.24, $\delta$ = 1.95, $\mu$ = -0.674, with 61 percent $\varphi$ = 18.605, $\gamma$ = -9.079, $\delta$ = 3.620, and $\mu$ = 0.149).

interpreted these pyroclastic-surge grain-size distributions as having saltation modes that are as fine-grained or finer than modes in aeolian and fluvial dunes. The saltation fractions from surge laminae exhibit log-hyperbolic distributions that are much more spread out (lower slopes $\varphi$ and $\gamma$ of the fine and coarse sides of the distributions). If moving air is the transport medium, the addition of fines and/or moisture may have affected the nature of ballistic collisions and resulting driving forces on the dominant grains, but the cumulative processes affecting transport and deposition of individual grains still generated hyperbolic saltation populations. Many fine-end limbs of the hyperbolic distributions have an order of magnitude more fine sand and silt (ash) than their aeolian and fluvial counterparts, but others have steeply decreasing amounts of fine sand and silt, similar to their aeolian and fluvial counterparts. These slopes on the fine end of the distribution curves must reflect the amount of removal of fine particles through suspension.

The parts of the distributions coarser than the saltation fraction may be creep components, similar to aeolian granule-megaripple distributions, but most are more similar to fluvial bedload distributions from gravelly megaripples. Some grain-size distributions have more coarse grains and larger clasts than would be driven by ballistic impacts of saltating grains. We suspect that these coarse grains may have moved as thin, granular basal shear flows mixed with an already existing saltation fraction, but the mechanics of moving such flows across preexisting dunes remains undetermined. Because of the similarity of the multi-modal distributions of coarse laminae from pyroclastic dunes and fluvial gravelly megaripples, the possibility that water was included as part of these basal shear flows cannot be ruled out.

The mixtures of hyperbolic saltation populations with coarser populations also raises questions about how they are mixed. The low slope values for the fine sides of the coarse populations do not appear to continue beyond the coarse limit of the saltation population, so are the two populations truncated where they meet or do they overlap at lesser logarithmic amounts?

Aeolian, some fluvial, and some pyroclastic-surge grain-size distributions exhibit hyperbolic shapes that can be modeled using four parameters. The hyperbolic parameters are different for the three kinds of deposits, with the slope of the two asymptotic lines ($\varphi$ and $\gamma$) more gentle for the pyroclastic-surge deposits. Because coarser modes in bimodal distributions do not occur by themselves, we cannot determine hyperbolic fits for them. However, mixtures of two hyperbolic models are able to reproduce bimodal distributions from Kilbourne and Hunts Holes (and other deposits of pyroclastic density currents). We suggest that such bimodal models have a slightly firmer physical basis (from aeolian and fluvial analogies) than previously proposed models using mixtures of several lognormal distributions (Wohletz, 1983; Wohletz et al., 1995).

## Acknowledgments

This project was initiated at the New Mexico Bureau of Mines and Mineral Resources under the direction of Dr. Frank Kottlowski. Dr. Gutjahr suggested that we do more work modeling the transport and deposition of the clasts, but the senior author was reassigned and Dr. Gutjahr became ill and died, so the project was put on a back shelf for years. We thank Bill Seager, Mike McCurry, Dana Bahar, and Ken Wolhetz for advice, field tours, and helpful discussions at Kilbourne and Hunts Holes. Dana Bahar provided some of the samples from Kilbourne Hole and sent her thesis to the senior author. We are grateful to Sylveen Robinson-Cook, Ghavan Mostafavi, Randy Roberts, Carol Rison, Mark Lund, Meredith Worden, Ellen Limburg, and Bob Friesen for help with the size analyses and reduction of computer data through the years. Bill Haneberg and Alex Rinehart graciously advised on computer manipulation of text and formulae. We are indebted to Bruce Allen for thoroughly reviewing several versions of the manuscript and suggesting many clarifying improvements. We are grateful to Dana Bahar and an anonymous reviewer for critical reviews that made this a much better and more comprehensive article. Becky Titus and Mickey Wooldridge drafted the graphs, and Leo Gabaldon provided additional drafting assistance.

## References


Allen, J.R.L., 1982, Sedimentary structures, their character and physical basis: Developments in Sedimentology, Part I, 30A and Part II, 30B: Elsevier, Amsterdam, p. A1-593; B1-663.

Anderson, R.S., 1990, Eolian ripples as examples of self-organization in geomorphological systems: Earth-Science Reviews, v. 29, p. 77–96.

Anderson, R.S, and Bunas, K.L., 1993, Grain size segregation and stratigraphy in aeolian ripples modelled with a cellular automaton: Nature, v. 365, p. 740–743.

Anderson, R.S., and Hallet, B., 1986, Sediment transport by wind: toward a general model: Geological Society of America Bulletin, v. 97, p. 523–535.

Andrews, B.J., and Manga, M., 2011, Effects of topography on pyroclastic density current runout and formation of coignimbrites: Geology, v. 39, p. 1099–1102.

Andrews, B.J., and Manga, M., 2012, Experimental study of turbulence, sedimentation and coignimbrite mass partitioning in dilute pyroclastic density currents: Journal of Volcanology and Geothermal Research, v. 225–226, p. 30–44.

Bagnold, R.A., 1937, The size grading of sand by wind: Proceedings of the Royal Society of London, Series A., v. 163, p. 252–564.

Bagnold, R.A., 1941, The physics of blown sand and desert dunes: Mehuen, London, 265 p.

Bagnold, R.A., 1966, An approach to the sediment transport problem from general physics: U.S. Geological Survey Professional Paper 422-I, 37 p.

Bagnold, R.A., 1968, Deposition in the process of hydraulic transport: Sedimentology, v.10, p. 45–56.

Bagnold, R.A., 1973, The nature of saltation and of bed-load transport in water: Proceedings of the Royal Society, Series A, v. 332, p. 473–504.

Bagnold, R.A., 1977, Bed-load transport by natural rivers: Water Resources Research, v. 13, p. 303–312.

Bagnold, R.A., 1979, Sediment transport by wind and water: Nordic Hydrology, v. 10, p. 309–322.

Bagnold, R.A., and Barndorff-Nielsen, O., 1980, The pattern of natural size distributions: Sedimentology, v. 27, p. 199–207.

Bahar, D., 1991, Evolution of the base surge deposits at Kilbourne Hole maar, south-central New Mexico [M.S. Thesis]: New Mexico State University, Las Cruces, 116 p.

Barndorff-Nielsen, O., 1977, Exponentially decreasing distributions for the logarithm of particle size: Proceedings of the Royal Society of London, Series A., v. 353, p. 401–419.

Barndorff-Nielsen, O., 1979, Models for non-Gaussian variation with applications to turbulence: Proceedings of the Royal Society of London, Series A., v. 368, p. 501–520.

Barndorff-Nielsen, O., Dalsgaard, K., Halgreen, C., Kuhlman, H., Moller, J.T., and Schou, G., 1982, Variation in particle size distribution over a small dune: Sedimentology, v. 29, p. 53–65.

Branney, M.J., and Kokelaar, P., 2002, Pyroclastic density currents and the sedimentation of ignimbrites: Geological Society of London, Memoir 27, 143 p.

Breard, E.C.P., and Lube, G., 2017, Inside pyroclastic density currents—uncovering the enigmatic flow structure and transport behavior in large-scale experiments: Earth and Planetary Science Letters, v. 458, p. 22–36.

Burgisser, A., and Bergantz, G.W., 2002, Reconciling pyroclastic flow and surge: the multiphase physics of pyroclastic density currents: Earth and Planetary Science Letters v. 202, p. 405–418.

Butterfield, G.R., 1999, Near-bed mass flux profiles in aeolian sand transport: high-resolution measurements in a wind tunnel: Earth Surface Processes and Landforms, v. 24, p. 393–412.

Cas, R.A.F., and Wright, J.V., 1987, Volcanic successions, modern and ancient: Allen and Unwin, London, 528 p.

Cole, P.D., 1991, Migration direction of sand-wave structures in pyroclastic surge deposits: implications for depositional processes: Geology, v. 19, p. 1108–1111.

Dellino, P., Isaia, P.R., and Veneruso, M., 2004, Turbulent boundary layer shear flows as an approximation of base surges at Campi Flegrei (southern Italy): Journal of Volcanology and Geothermal Research, v.133, p. 211–228.

Dellino, P., Mele, D., Sulpizio, R., La Volpe, L., and Braia, G., 2008, A method for the calculation of the impact parameters of dilute pyroclastic density currents based on deposit particle characteristics: Journal of Geophysical Research, v. 113, p. B7206–7227.

Dong, Z., Liu, X., Wang, H., Zhao, A., and Wang, X., 2002, The flux profile of a slowing sand cloud: a wind tunnel investigation: Geomorphology, v. 49, p. 219–230.

Doronzo, D.M., and Dellino, P., 2011, Interaction between pyroclastic density currents and buildings: Numerical simulation and first experiments: Earth and Planetary Science Letters, v. 310, p. 286–292.

Douillet, G.A., Pacheco, D.A., Kueppers, U., Letort, J., Tsang-Hin-Sun, E., Bustillos, J., Hall, M.,Ramon, P., and Dingwell, D.B., 2013, Dune bedforms produced by dilute pyroclastic density currents from the August 2006 eruption of Tungurahua volcano, Ecuador: Bulletin of Volcanology, v. 75:762, 20 p.

Douillet, G.A., Rasumssen K.R., Kueppers, U. Lo Castro, D., Merrison, J.P., Iversen, J.J. and Dingwell, 2014, Saltation threshold for pyroclasts at various bedslopes: Wind tunnel measurements: Journal of Volcanology and Geothermal Research, v. 278–279, p. 14–24.

Douillet, G.A., Taisne, B, Tsang-Hin-Sun, E., Muller, S.K., Kueppers, U., and Dingwell, D.B., 2015, Syn-eruptive, soft-sediment deformation of deposits from dilute pyroclastic density current: triggers from granular shear, dynamic pore pressure, ballistic impacts and shock waves: Solid Earth, v. 6, p. 553–572.

Duran, O., Claudin, P., and Andreotti, B., 2011, On aeolian transport: grain-scale interactions, dynamical mechanisms and scaling laws: Aeolian Research, v. 3, p. 243–270.

Eychenne, J., Le Penec, J.L., Troncoso, L., Gouhier, M., and Nedelec, J.M., 2012, Causes and consequences of bimodal grain-size distributions of tephra deposited during the August 2006, Tungurahua eruption (Ecuador): Bulletin of Volcanology, v. 74, p. 187–205.

Farrell, E.J., Sherman, D.J., Ellis, J.T., and Li, B., 2012, Vertical distribution of grain size for wind blown sand: Aeolian Research, v. 7, p. 51–61.

Fisher, R.V., 1970, Base surge bed forms in maar volcanoes: American Journal Science, v. 268, pp. 157–180.

Fourriere, A., Claudin, P., and Andreotti, B., 2010, Bedforms in a turbulent stream: formation of ripples by primary linear instability and of dunes by nonlinear pattern coarsening: Journal of Fluid Mechanics, v. 649, p. 287–328.

Gile, L.H., 1987, A pedogenic chronology for Kilbourne Hole, southern New Mexico-II: time of the explosions and soil events before the explosions: Journal of the Soil Science Society of America, v. 51, p. 746–760.

Gencalioglu-Kuscu, G. Atilla, C., Cas, R.A.F., and Kuscu, I., 2007, Base surge deposits, eruption history, and depositional processes of a wet phreatomagmatic volcano in Central Anatolia (Cora Maar): Journal of Volcanology and Geothermal Research, v. 159, p. 198–209.

Girolami, L., Druitt, T.H., and Roche O., 2015, Towards a quantitative understanding of pyroclastic flows: effects of expansion on the dynamics of laboratory fluidized granular flows: Journal of Volcanology and Geothermal Research, v. 296, p. 31–39.

Gravina, T., Lirera, L., Marzocchella, A., Petrosinoa, P., and Salatinob, P., 2004, Fluidization and attrition of pyroclastic granular solids: Journal of Volcanology and Geothermal Research, v. 147, p. 27–42.

Ho, T.D., Valance, A., Dupont, P., and El Moctar, A.O., 2014, Aeolian sand transport: length and height distributions of saltation trajectories: Aeolian Research, v. 12, p. 65–74.

Houghton, B.F., Wilson, C.J.N., Smith, R.T., and Gilbert J.S., 2000, Phreatoplinian eruptions: *in* H. Sigurdsson, B. Houghton, S.R. McNutt, H. Rymer, and J. Stix, eds., Encyclopedia of Volcanoes: Academic Press, London, p. 513–525.

Hunter, R.E., 1977, Basic types of stratification in small eolian dunes: Sedimentology, v. 24, p. 361–387.

Janebo, M.H., Houghton, B.F., Thordarson, T., Bonadonna, C., and Carey, R.J., 2018, Total grain-size distribution of four subplinian-Plinian tephras from Hekla volcano, Iceland: implications for sedimentation dynamics and eruption source parameters: Journal of Volcanology and Geothermal Research, v. 357, p. 25–38.

Kok, J.F., Parteli, E.J.R., Michaels, T.I., and Karam, D.B., 2012, The physics of wind-blown sand and dust: Reports on Progress in Physics, v. 75, 72 p.

Kuester, J.L., and Mize, J.H., 1973, Optimization techniques with Fortran: McGraw-Hill, New York, 500 p.

Lorenz, V., 1973, On the formation of maars: Bulletin Volcanologique, v. 37, p. 183–204.

Love, D.W., Boyle, J.T., Robinson, S., and Hemingway, M., 1985, Location-dependent sediment sorting in gravelly megaripples from the Rio Grande, central New Mexico: New Mexico Geology, v. 7, pp. 26–30.

Love, D.W., Gutjahr, A., and Robinson-Cook, S., 1987, Location-dependent sediment sorting in bedforms under waning flow in the Rio Grande, central New Mexico: Society for Economic Paleontologists and Mineralogists, Special Publication 39, p. 37–47.

Mayaud, J.R., Bailey, R.M., Wiggs, G.F.S., and Weaver, C.M., 2017, Modelling aeolian sand transport using a dynamic mass balancing approach: Geomorphology, v, 280, p. 108–121.

Moore, J.G., 1967, Base surge in recent volcanic eruptions: Bulletin of Volcanology, v. 30, p. 337–363.

Namikas, S.L., 2003, Field measurement and numerical modelling of aeolian mass flux distributions on a sandy beach: Sedimentology, v. 50, p. 303–326.

Namikas, S.L., 2006, A conceptual model of energy partitioning in the collision of saltating grains with an unconsolidated sediment bed: Journal of Coastal Research, v. 22, p. 1250–1259.

Qian, G., Dong, Z., Zhang, Z., Luo, W., and Lu, J., 2012, Granule ripples in the Kumtagh Desert, China: morphology, grain size, and influencing factors: Sedimentology, v. 59, p. 1888–1901.

Rasmussen, K.R., Iversen, J.D., and Rautahemio, P., 1996, Saltation and wind-flow interaction in a variable slope wind tunnel: Geomorphology, v. 17, p. 19–28.

Rasmussen, K.R., Valance, A., and Merrison, J., 2015, Laboratory studies of aeolian sediment transport processes on planetary surfaces: Geomorphology, v. 344, p. 74–94.

Rice, M.A., Willetts, B.B., and McEwan, I.K., 1995, An experimental study of multiple grain-size ejecta produced by collisions of saltation grains with a flat bed: Sedimentology, v. 42, p. 695–706.

Reineck, H.E., and Singh, I.B., 1980, Depositional sedimentary environments: Springer-Verlag, New York, 549 p.

Roche, O., Gilbertson, M.A., Phillips, J.C., and Sparks, R.S.J., 2004, Experimental study of gas-fluidized granular flows with implications for pyroclastic flow emplacement, Journal of Geophysical Research, v.109, B10201, 14 p.

Rowley, P.D., MacLeod, N.S., Kuntz, M.A., and Kaplan, A.M., 1985, Proximal bedded deposits related to pyroclastic flows of May 18, 1980 Mount St. Helens, Washington: Geological Society of America Bulletin, v. 96, p. 1373–1383.

Seager, W.R., 1987, Caldera-like collapse at Kilbourne Hole Maar, New Mexico: New Mexico Geology, v. 9, p. 69–73.

Sheridan, M.F., and Wohletz, K.H., 1983, Hydrovolcanism: basic considerations and review: Journal of Volcanology and Geothermal Research, v. 17, p. 1–29.

Sheridan, M.F., Wohletz, K.H., and Dehn, J., 1987, Discrimination of grain-size subpopulations in pyroclastic deposits: Geology, v. 15, p. 367–370.

Sohn, Y.K., 1997, On traction-carpet sedimentation: Journal of Sedimentary Research, v. 67, p. 502–509.

Sohn, Y.K., and Chough, S.K., 1989, Depositional processes of the Suwolbong Tuff Ring, Cheju Island (Korea): Sedimentology, v. 36, p. 837–855.

Stuart, C.J., 1981, Hunt's Hole maar volcano, Dona Ana County, south-central New Mexico: El Paso Geological Society Guidebook, 1981 field conference, p. 64–72.

Stuart, C.J., and Brenner, M.G., 1979, "Low-regime" base surge dunes—an example from Kilbourne and Hunts Holes, south-central New Mexico [abstract]: Geological Society of America Abstracts with Programs, v. 11, p. 525.

Sulpizio, R., Dellino, P., Doronzo, D.M., and Sarocchi, D., 2014, Pyroclastic density currents: state of the art and perspectives: Journal of Volcanology and Geothermal Research, v. 283, p. 36–65.

Thorarinsson, S., 1967, Surtsey: The new island in the north Atlantic: Viking, New York, 47 p.

Valance, A., Rasmussen, K.R., El Moctar, A.O., and Dupont, P., 2015, The physics of aeolian sand transport: Comptes Rendus Physique, Granular physics, v. 16, p. 105–117.

Valentine, G.A., and Fisher, R.V., 2000, Pyroclastic surges and blasts: *in* H. Sigurdsson, B. Houghton, S.R. McNutt, H. Rymer, and J. Stix, eds., Encyclopedia of Volcanoes, Academic Press, London, p. 571–580.

Valentine, G.A., Sottili, G., Palladino, D.M., and Taddeucci, J., 2015, Tephra ring interpretation in light of evolving maar-diatreme concepts: Stracciacappa maar (central Italy): Journal of Volcanology and Geothermal Research, v. 308, p. 19–29.

Vespermann, D., and Schmincke, H.U., 2000, Scoria cones and tuff rings: *in* H. Sigurdsson, B. Houghton, S.R. McNutt, H. Rymer, and J. Stix, eds., Encyclopedia of Volcanoes, Academic Press, London, p. 683–694.

Waters, A.C., and Fisher, R.V., 1971, Base surges and their deposits: Capelinhos and Taal volcanoes: Journal of Geophysical Research, v. 76, p. 5596–5614.

Walker, G.P.L., 1983, Ignimbrite types and ignimbrite problems: Journal of Volcanology and Geothermal Research, v. 17, p. 65–88.

Walker, G.P.L., 1984, Characteristics of dune-bedded pyroclastic surge bedsets: Journal of Volcanology and Geothermal Research, v. 20, p. 281–296.

White, J.D.L., and Houghton, B., 2000, Surtseyan and related phreatomagmatic eruptions: *in* H. Sigurdsson, B. Houghton, S.R. McNutt, H. Rymer, and J. Stix, eds., Encyclopedia of Volcanoes, Academic Press, London, p. 495–511.

White, J.D.L., and Ross, P.S., 2011, Maar-diatreme volcanoes: a review: Journal of Volcanology and Geothermal Research, v. 201, p. 1–29.

Williams, G., 1964, Some aspects of the eolian saltation load: Sedimentology, v. 3, p. 257–287.

Wilson, C.J.N., 1980. The role of fluidization in the emplacement of pyroclastic flows: Journal of Volcanology and Geothermal Research, v. 8, p. 231–249.

Wilson, C.J.N., 1984. The role of fluidization in the emplacement of pyroclastic flow 2: experimental results and their interpretation: Journal of Volcanology and Geothermal Research, v. 20, p. 55–78.

Wohletz, K.H., 1980, Explosive hydromagmatic volcanism [Ph.D. dissertation]: Arizona State University, Tempe, Arizona, 303 p.

Wohletz, K.H., 1983, Mechanisms of hydrovolcanic pyroclast formation: grain-size, scanning electron microscopy, and experimental studies: Journal of Volcanology and Geothermal Research, v. 17, p. 31–63.

Wohletz, K.H., Orsi, G., and Vota. S., 1995, Eruptive mechanisms of the Neapolitan Yellow Tuff interpreted from stratigraphic, chemical, and granulometric data: Journal of Volcanology and Geothermal Research, v. 67, p. 263–290.

Yizhaq, H., 2008, Aeolian megaripples: mathematical model and numerical simulations: Journal of Coastal Research, v. 24, p. 1369–1378.

Zou, X.Y., Wang, Z.L., Hao, Q.Z., Z. C.L., Liu, Y.Z., and Dong, G.R., 2001, The distribution of velocity and energy of saltating sand grains in a wind tunnel: Geomorphology, v. 36, p. 155–165.